International Journal of GEOMATE, January, 2024 Vol.26, Issue 113, pp.115-122
ISSN: 2186-2982 (P), 2186-2990 (O), Japan, DOI: https://doi.org/10.21660/2024.113.g13375
Geotechnique, Construction Materials and Environment

MODELLING OF FLOW AND SCOUR AROUND THE PIERS WITH DIFFERENT GEOMETRIC SHAPES

*Dhemi Harlan[1], Ilmiadin Rasyid[2], Joko Nugroho[1], Mohammad Bagus Adityawan[1] and Dantje Kardana Natakusumah[1]

[1]Faculty of Civil and Environmental Engineering, Institut Teknologi Bandung, Indonesia;
[2]Water Resource Engineering Postgraduate Alumni, Institut Teknologi Bandung, Indonesia

*Corresponding Author, Received: 09 Jul. 2023, Revised: 15 Dec. 2023, Accepted: 09 Jan. 2024

ABSTRACT: The piers of the bridge can change the flow pattern in the river. This means the hydraulic conditions of the river can be changed, including the increased shear stress at the bottom of the river or natural channel that has the potential to cause scour. The investigation of the flow pattern around the piers on the channel is needed to consider which parts of the piers are sensitive to scour and to analyze the flow phenomena around the piers. So, this study will investigate the flow and its effect on the scour around the piers with different geometric shapes. This study uses a fluid flow model coupled to the sediment scour model, including the Meyer Peter Muller sediment transport equation. The result of this study was obtained for one circular pier; the bed load calibration parameter was 8, and the channel roughness calibration parameter was 2.5. The calculations of scour height, scour angle and flow have a fairly good similarity. Then, these calibration parameters are used to simulate flow and scour on two circular piers, two circular end piers, and two triangular end piers. The modeling results show that there are maximum scours with the same depth of 0.04 m, but the scouring patterns are different. The maximum shear stresses obtained successively by two circular end piers, two triangular end piers, and two circular piers are 0.315 N/ m2, 0.366 N/ m2, and 0.29 N/ m^2. Two circular piers give a better result than two circular end piers and two triangular piers.

Keywords: Flow, Scour, Sediment transport, Piers, Geometric

1. INTRODUCTION

Generally, the bridge is completed with the piers and abutments on the left and right of the river bank. One important part of the bridge is the piers. The piers are the supporting structure of the bridge that continues the forces that support the bridge to the ground. Based on observation, the piers have variations of shapes and numbers. They depend on the load it supports, aesthetics, and other structural considerations.

Bridge scour refers to the process of sediment removal, sand, and gravel around the foundations of bridges known as abutments or piers. This erosion occurs due to the flow of water. It can have detrimental effects on the integrity of a bridge. Scouring poses a risk to bridge stability as it is responsible for 60% of bridge failures in the United States [1]. The alteration in water flow patterns around these structures leads to changes in flow velocities ultimately resulting in the creation of scour holes around them. Multiple factors influence this process, including flow depth, angles, currents and the shape of piers and abutments. Monitoring scouring's challenging and foundation failure caused by scour can occur without any warning signs. To mitigate this issue various methods are employed to minimize the scouring impact on bridge piers. When designing a bridge structure addressing stream stability and implementing measures, against scouring becomes crucial.

There are forms of bridge scouring including local scour, general scour, and contraction scour. Local Scour is the type of scour where sediment is removed from, around bridge piers or abutments resulting in the formation of scour holes. It can be further divided into clear water scour and live bed scour. General Scour refers to the decrease in the riverbed elevation. It usually happens over a short period. While contraction scour occurs when there is a narrowing of the flow area, which leads to increased flow velocities and subsequent scouring. These different types of scour can pose a risk to bridge stability. Therefore, it is crucial to understand and monitor them closely in order to minimize their impact.

Bridge scouring, which refers to the erosion of soil, around bridge piers and abutments caused by water flow can occur due to factors including flow patterns, water currents, sediment properties, debris, and stream channel instability. When a bridge is constructed over a river unique flow patterns emerge around the piers and abutments. The presence of these structures alters the flow velocities leading to the formation of scour holes. Water currents during floods can cause hydrodynamic scouring that carves out scour holes and poses a risk to the integrity of the bridge. The type of sediment surrounding the foundation of a bridge can influence its susceptibility to scouring. Loose alluvial material is particularly

prone to erosion. Debris can impact bridge scour in ways, such as reducing the size of the waterway beneath a bridge, increasing obstruction area, and altering the direction of water flow. These factors contribute to scour. River erosion and changes in angles of attack resulting from stream channel instability can also play a role in causing bridge scour. Addressing these causes is crucial, during the design and monitoring phases of bridges to effectively mitigate the risk of scouring and ensure long-term stability.

The piers of the bridge can cause the river flow to change, so this means the hydraulics of the river will be changed. The shear stress will be increased on the bed of the river, and this triggers the potential for scour. Sediment transport will increase with increasing sediment shear stress. Scour occurs when changes in flow conditions cause an increase in the bed shear stress, according to [2]. This condition is given in the sediment transport equation [3,4,5,6] when the shear stress of flow is greater than critical shear stress, so this situation will cause sediment transport. If the flow shear stress is below critical shear stress, it will not cause scour.

The pier placed in a river current is able to change the water flow and vertical velocity gradient [7]. The flow beneath the pier forms a vortex that eventually sweeps around and beneath the structure. This event is called a horseshoe vortex because, when viewed from above, the vortex has the shape of a horseshoe.

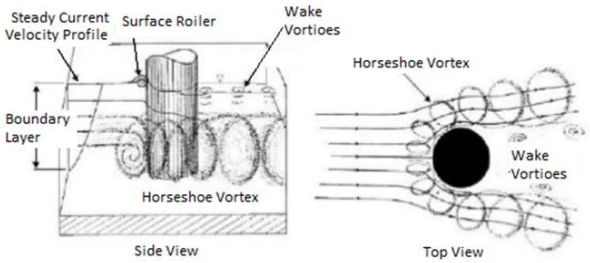

Fig.1 Scour Mechanism [7]

The shear stress generally increases at the bottom of the channel at the front of the pier. If the bottom of the channel is easily eroded, scour holes will form around the pier. This is what is called local scour [7]. The scouring process begins when particles are moved following the flow pattern from upstream to downstream of the channel. At high velocity of flow, the particles carried will increase and make the size and depth of the scour hole become larger. If the flow velocity reaches a critical speed, the scour depth will be maximum.

2. RESEARCH SIGNIFICANCE

The investigation of scour phenomena around the pier in the river or channel is needed to understand how the flow in the channel or river will gradually trigger and affect the scour around the pier, as shown in [8]. Regarding the design of piers, how the different geometrics of piers can give effect to the scour and to the parameter of flow pattern around the piers, and to select the best geometric of the pier. This investigation will be expected to provide benefits for practitioners in determining the pier designs that are safe from scour. Additionally, it will give information for the next researchers to improve the understanding of scour phenomena around the piers through numerical modeling in further investigation.

3. MATHEMATICAL FORMULATION

The differential equations to be solved are written in terms of Cartesian coordinates (x, y, z) . All equations are formulated with area and volume porosity functions. This formulation is called the Fractional Area-Volume Obstacle Representation (FAVOR) Method, used to model complex geometric regions [9].

The sediment scour model is fully coupled with fluid flow, allows multiple non-cohesive species, and considers entrainment, deposition, bed load transport, and suspended load transport. This model is described by the FAVOR technique, and area and volume fractions describing the sediment model are calculated throughout the domain at each time.

3.1 Fluid Flow Model

The flow can be modelled by using continuity equation, momentum equation, and the volume of fluid equation in Cartesian coordinate [9,10]. These equations are presented in equation 1 to 3 below.

$$\frac{V_F}{\rho c^2}\frac{\partial p}{\partial t} + \frac{\partial}{\partial x}(uA_x) + R\frac{\partial}{\partial y}(uA_y) + \frac{\partial}{\partial z}(uA_z) = \frac{R_{SOR}}{\rho} \quad (1)$$

$$\frac{\partial u}{\partial t} + \frac{1}{V_F}\left\{uA_x\frac{\partial u}{\partial y} + vA_yR\frac{\partial u}{\partial y} + wA_z\frac{\partial u}{\partial z}\right\} = -\frac{1}{\rho}\frac{\partial p}{\partial x} + G_x + f_x - b_x - \frac{R_{SOR}}{\rho V_F}(u - u_w - \delta u_s)$$

$$\frac{\partial v}{\partial t} + \frac{1}{V_F}\left\{uA_x\frac{\partial v}{\partial y} + vA_yR\frac{\partial v}{\partial y} + wA_z\frac{\partial v}{\partial z}\right\} = -\frac{1}{\rho}\left(R\frac{\partial p}{\partial y}\right) + G_y + f_y - b_y - \frac{R_{SOR}}{\rho V_F}(v - v_w - \delta v_s)$$

$$\frac{\partial w}{\partial t} + \frac{1}{V_F}\left\{uA_x\frac{\partial w}{\partial y} + vA_yR\frac{\partial w}{\partial y} + wA_z\frac{\partial w}{\partial z}\right\} = -\frac{1}{\rho}\frac{\partial p}{\partial z} + G_z + f_z - b_z - \frac{R_{SOR}}{\rho V_F}(w - w_w - \delta w_s) \quad (2)$$

$$\frac{\partial F}{\partial t} + \frac{1}{V_F}\left[\frac{\partial}{\partial x}(FA_xu) + R\frac{\partial}{\partial y}(FA_yv) + \frac{\partial}{\partial z}(FA_zw)\right] = F_{SOR} \quad (3)$$

Where V_F is the fractional volume open to flow, ρ is the fluid density, c^2 is the square of the sound speed,

and R_{SOR} is a mass source. The velocity components (u, v, w) are in the coordinate directions (x, y, z) or (r, R_{SOR}, z) . A_x is the fractional area open to flow in the x-direction, and A_y , A_z are similar area fractions for flow in the y and z directions, respectively. The coefficient R depends on the choice of coordinate system in the following way. When cylindrical coordinates are used, derivatives must be converted to azimuth derivatives.

In these equations, (G_x , G_y , G_z) are body accelerations, (f_x , f_y , f_z) are viscous accelerations, and (b_x , b_y , b_z) are flow losses in porous media or across porous baffle plates, and the final terms account for the injection of mass at a source represented by a geometry component.

The term $U_w = (u_w, v_w , w_w)$ in Equation (2) is the velocity of the source component, which will generally be non-zero for a mass source at a General Moving Objects Model. Meanwhile the term $U_s = (u_s , v_s , w_s)$ is the velocity of the fluid at the surface of the source relative to the source itself.

3.2 Bed Load Transport

The morphological change related to the thickness eroded sediment is given by using Exner sediment continuity equation as following below.

$$\frac{\partial z}{\partial t} + \xi \nabla \cdot q_s = 0 \tag{4}$$

Where z is a bottom elevation, $\xi = (1-P)^{-1}$ where P is a porosity, and q_s is a bed sediment flux.

Bed sediment flux in a dimensionless form as shown in [11] is computed by using Meyer-Peter and Muller equation as below.

$$q_s^* = B(\theta - \theta_c)^{1,5} \tag{5}$$

Where B is a bed load factor, θ and θ_c are Shields and critical Shields parameters. Critical Shields can be determined from the equation in [12]. Both can be written in a dimensionless form as

$$\theta = \frac{\tau}{gd(s-1)} \quad , \quad \theta_c = \frac{\tau_c}{gd(s-1)} \tag{6}$$

Here τ and τ_c are a shear stress at the bed and a critical shear stress, g is a gravity in absolute value, d is a grain diameter, and $s = \rho/\rho_f$ is a specific weight of sediment, ρ is the mass density of sediment grains. The dimensionless form of bed sediment flux can be defined as

$$q_s^* = \frac{q_s}{[gd^3(s-1)]^{1/2}} \tag{7}$$

The flow creates the forces that these tend to move or drag base layer grains [13]. When the force acting on sediment grains reaches a certain value, so that if a little force is added it will cause the sediment grains to move, then this condition is called a critical condition.

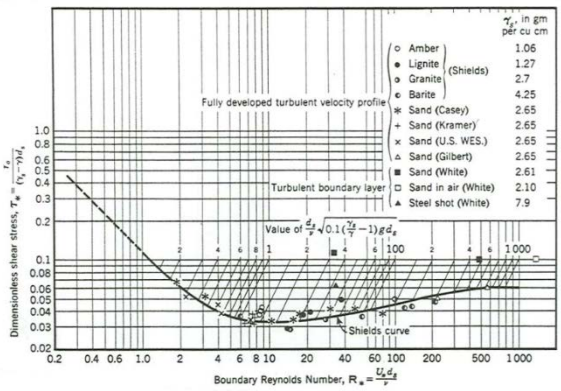

Fig.2 Shield Graphic [14]

Fig. 2 shows the Shields curve, by finding out Reynold Number (Re) of grain or grain diameter (d_{50}), so the critical shear stress (τ_c) value can be obtained. When the bed shear stress of flow is above the critical value then the sediment grains move.

3.3 Suspended Load Transport

Suspended load transport equation is given by following equation

$$\frac{\partial C_s}{\partial t} + \nabla \cdot (u_s C_s) = \nabla \cdot \nabla (D C_s) \tag{8}$$

Where C_s is suspended sediment mass concentration, D is diffusivity, and u_s is the sediment velocity. Computation of erosions includes sediment entrainment and deposition simultaneously. The lifting velocity of grains in entrainment employs the equation in [15]. The settling velocity calculation uses equation in [16] for deposition and suspended load transport.

3.4 Empirical Scour Equation

Colorado State University (CSU) equation is the most widely used equation in America [17]. It is given as

$$\frac{h_s}{h_1} = 2 \times \left(\frac{D}{h_1}\right)^{0,65} \times Fr^{0,43} \tag{9}$$

The equation for the calculation of scour depth based on data of sediment transport study case result is explained in [18]. The factors that influence the maximum local scour depth include pier shape, sediment gradation, and flow angle. The equation is given as below.

$$h_s = 1{,}35\, D^{0,7}\, h_1{}^{0,3} \tag{10}$$

The equation of pier scour based on experiment [19] is given as:

$$h_s = D\ k_\alpha k_I k_y k_{\mu 4} k_\sigma \quad (11)$$

Sediment gradation coefficient $(k_\sigma = 1{,}0)$ and flow intensity coefficient (k_I) use the equation as below.

$$k_I = \begin{cases} 2{,}4\ (V/V_c)^{0{,}255} & V < V_c \\ 2{,}4 & V > V_c \end{cases} \quad (12)$$

Where $V_c = 5{,}75 u_{*c} log(5{,}53 h_1/D_{50})$

The flow depth coefficient (k_y) uses the equation of

$$k_y = \begin{cases} 0{,}78\ (h_1/D)^{0{,}255} & untuk\ h_1/D < 2{,}6 \\ 1{,}0 & untuk\ h_1/D > 2{,}6 \end{cases} \quad (13)$$

The sediment size coefficient is

$$k_{\mu 4} = \begin{cases} 0{,}78\ (h_1/D)^{0{,}255} & untuk\ D/D_{50} < 25 \\ 1{,}0 & untuk\ D/D_{50} > 25 \end{cases} \quad (14)$$

4. RESULT AND DISCUSSION

Calibration of model result is the activity to obtain appropriate coefficients in the model input to find the best solution. This can be achieved by comparing with previous observation investigation by physical model test in laboratory or analytical solution. In this study, physical model test used as comparison was done in [20]. This has the objective to calibrate and validate the result of scour model by using FLOW-3D.

This physical model used the flume with the length of 155.88 cm, the height of 50 cm, and the width of 45.6 cm. A circular pier was placed in the center of flume channel. It had the diameter of 5.08 cm. The velocity of flow during physical model test was 0.25 m/s with the water depth of 15 cm. The time of simulation required 30 minutes to get stable results. The layout of physical model test was illustrated as following below.

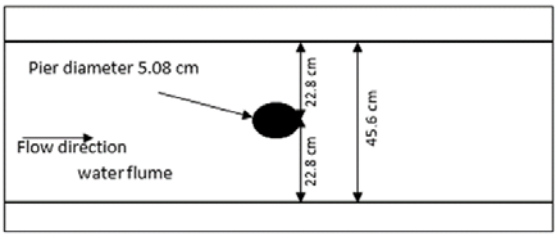

Fig.3 Layout of physical model test [20]

4.1 Model Test

While numerical model in this study uses domain with the length of 40D (D = 5.08 cm). The composition along x direction consists of the first of 6.5D for solid material, the middle of 29D cm for sediment material, and the last of 4.5D for solid material. The domain has the width of 45 cm, the bed material thickness of 20 cm and the height from the bed surface of 40 cm. Outlet is placed with the distance of 18.5D from downstream of pier. Other parameters are used in this model as Table 1 below.

Table 1 Scour model parameters

Parameter	Value
Length	2.032 m
Width	0.45 m
d_{50}	0.385 mm
Water Depth	0.15 m
Velocity	0.25 m/s
Diameter of Pier	5.08 cm
Mesh	10 – 20 mm

In numerical model, meshing has a significant role to get a good solution. The mesh is considered as one factor that can influence simulation process and can change the time operation depending on number of nodes and elements. Various the size of mesh has been checked to get which mesh will give a good result. In this study, the size of mesh selected is 10 mm to 20 mm as shown below.

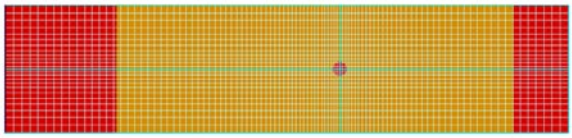

Fig.4 Mesh of domain

Determining the appropriate boundary conditions before carrying out the simulation is very important to get an accurate solution. The boundary conditions are applied to numerical model and some parameters that give effect directly are calibrated by comparing to previous physical model test to get a good result. Then calibrated parameters can be applied to numerical simulation.

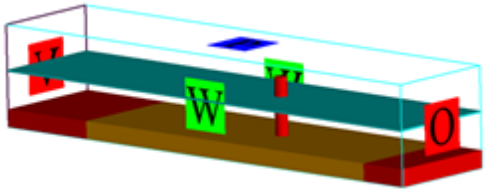

Fig.5 Boundary conditions on domain

As shown in Fig.5 above, inlet boundary is velocity (V) of 0.25 m/s, initial water depth of 0.15 m. Downstream of channel is free outflow (O), while

wall boundary (W) is obtained on the left and the right sides. Then the pressure boundary (P) is applied above domain of model.

In this model, it uses the equation Soulsby-Whitehouse to obtain critical shields. The coefficient of the comparison between channel roughness and d_{50} , K/d_{50} , in this model will be tried for 1, 2, and 2.5. Meyer-Peter and Muller bed load equation is used with bed load coefficient range of 1 to 13. Then entrainment coefficient is tried between 0.018 and 0.18. The duration of simulation is 30 minutes.

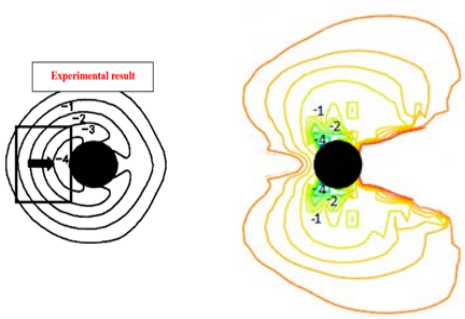

Fig.6 Comparison between Physic model (left) in [20] and numerical model (right)

The result of simulation after 30 minutes by trial and error is shown on the right in Fig.6, with the coefficient K/d_{50} of 2.5, the bed load coefficient of 8, and entrainment coefficient of 0.09. The scour pattern occurs around the pier.

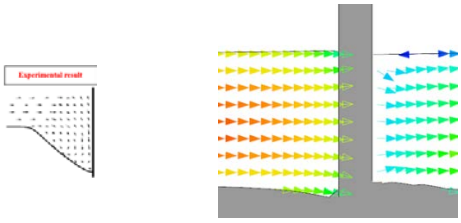

Fig.7 The flow on the local scour hole (physical model on the left and numerical model on the right)

Fig.7 shows the contour of scour hole after 30 minutes. The maximum scour depth is around 4 cm as same as physical model as shown in Table 5, but the morphology of scour hole is quite different. While the scour holes of empirical results (Colorado State University, CSU, Laursen and Torch, LT, Menville and Sutherland, MS) give the depth of twice than numerical and experimental results.

Table 2 Results of numerical model to physical model and empirical calculation results.

Empirical (m)			Experim ental (m)	Numeri cal (m)
CSU	LT	MS		
0.075	0.081	0.095	0.04	0.04

The depth of maximum scour occurs on two sides of piers, while the physical model result is in front of the pier. This occurs on FLOW-3D model result because there is no function of sediment collapse, hence sediment is only eroded when the flow shear stress is high.

4.2 Model Application

Based on the parameters that are found in calibration process, we use those parameters for the simulations in the cases of two piers with various geometric shapes. Cases are used in this study consist of two piers with circular shapes, two piers with triangular ends, and two piers with circular ends.

The first case is a channel having two piers with circular shapes, the diameter of each pier is D, the distance between two piers is 2D. Second case has two piers with sharp ends with the length of 4D. While, the last case has two piers with circular ends.

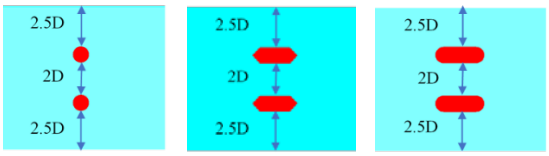

Fig.8 Various geometrics of piers

The meshes are used having 48,480 grids and the size with the range of 1 cm to 2 cm. The meshes around the piers with the smallest mesh size. This will be useful to check the flow and scour in detail of the model simulation results.

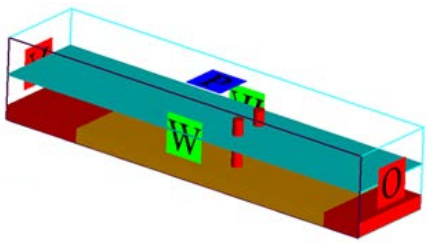

Fig.9 Domain of two piers with circular shapes

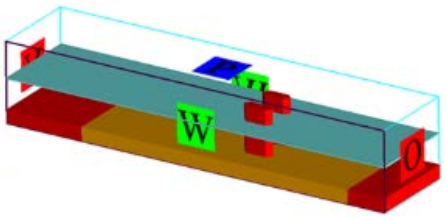

Fig.10 Domain of two piers with sharp ends

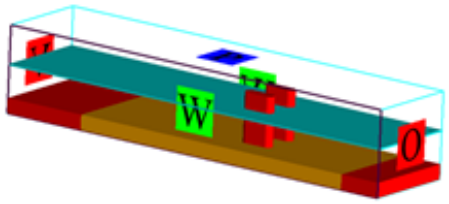

Fig.11 Domain of two piers with circular ends

4.2.1 The Flow Velocity Pattern

Fig.12 shows that the maximum velocity pattern every model result is different. On two piers with circular and circular ends shapes have the velocities of right and left sides with the same velocity of 0.25 m/s. While the velocity of two piers with sharp ends gives 0.28 m/s on the area between two piers. This is caused by the shapes of piers that direct the flow to the area between the piers.

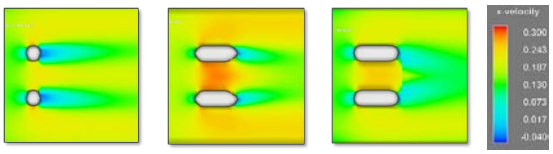

Fig.12 The flow velocity pattern

On the back of the piers. all models have a deceleration, sequentially they are two piers with circular ends, two circular piers, and with sharp ends. No backflow occurs behind the piers with circular ends because the flow velocity is low, hence the side flow is not enough energy to follow the geometry of the piers. Then the side flow is pushed up by the flow behind it. This occurs the same as the piers with triangular ends, it is no backflow due to sharp rear piers geometry.

4.2.2 Froude Number

Fig.13 shows that on the two circular piers and two circular ends piers have quite similar Froude number of 0.181 and 0.184. While on the two triangular ends piers has maximum Froude number of 0.21 in the area between the piers (inside part) and maximum Froude number of 0.2 outside part of the piers.

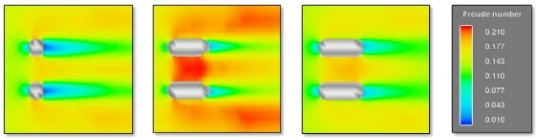

Fig.13 The Froude Number pattern

In front of all models results has lower Froude number than average Froude number because the flow is restrained by the piers thereby reducing the flow velocity and then reducing the Froude number. The minimum Froude number of 0.01 is shown in Fig.13 behind two circular piers. This is caused the incoming flow divided in two directions of left and right around a spherical geometry, then the flow from the left and the right side meet each other on the rear of the piers hence creating a counterclockwise flow. While the Froude number behind piers with circular ends is lower with the area bigger than the piers with sharp ends.

4.2.3 Bed Shear Stress Pattern

Fig.14 shows that the shear stress on two piers model with triangular ends has influenced area of stress behind the piers quite high with the maximum shear stress of 0.366 N/m^2. While two circular piers have 0.29 N/m^2 and two circular ends piers have 0.315 N/m^2.

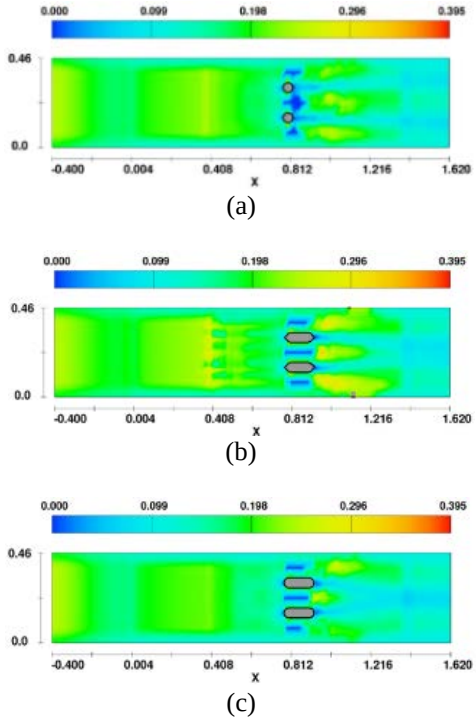

Fig.14 The bed shear stress pattern

4.2.4 Scour Pattern

Fig.15 shows the pattern of scour and cross section of model for every type of piers. On circular piers model result shows the deepest scour on circular piers is 4 cm, same as the piers with circular ends and with triangular ends. Outside part of piers with circular ends and triangular ends tend to get the same area of scour, while inside part of piers seems that the scour under elevation of zero on the piers with triangular ends has a bigger area.

Fig.15 (a) and (c) on the right (cross section) show that the scours of two circular piers and two circular ends piers tend to have a convex curve in the area between the piers. While in Fig.15 (b), the scour of two triangular ends piers has a concave curve and deeper. This is due to the flow velocity inside

triangular piers is higher and giving higher shear stress than two other models.

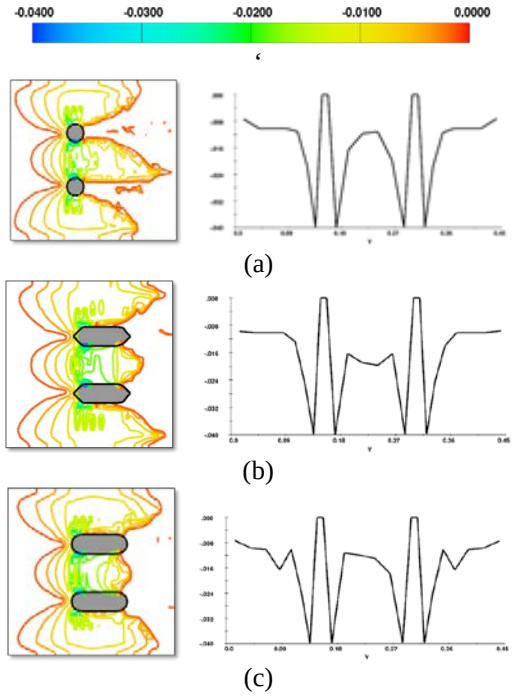

Fig.15 The bed scour pattern and cross section

5. CONCLUSION

All simulations of sediment transport processes of non-cohesive soil, bed load transport, suspended load transport, entrainment, and deposition employ fully-coupled of fluid dynamics and sediment scour model in FLOW-3D.

One circular pier is employed for model calibration and found the ratio of channel roughness and sediment grain, K/d_{50} of 2.5 and bed load coefficient of 8. The calculation of scour height, scour angle and flow have a fairly good similarity. While, topography of scour is not quite similar because in this model, there is no collapse sediment function, hence the scour is not rounded in front of the piers as experiment result for low shear stress.

The model by using parameters of calibration result for one pier is applied to scour around two rounded piers, two triangular ends piers, and two rounded ends piers. All models of two piers with various shapes show the subcritical flow. The triangular ends piers have the biggest Froude Number of 0.21 inside part of piers and it tends to give the deeper scour compared to two other models.

The modeling results show that there are maximum scours with the same depth of 0.04 m, but the scouring patterns are different. Based on the comparison of maximum shear stress values, two circular piers with the value of 0.29 N/m^2 give less scour than two circular ends piers with 0.315 N/m^2, and two triangular piers with 0.366 N/m^2. This means two circular piers give better result than two others.

6. ACKNOWLEDGMENTS

This work is supported by the Faculty of Civil and Environmental Engineering, ITB through The Program of Research, Community Service, and Innovation for Research Division ITB (P2MI ITB).

7. REFERENCES

[1] FHWA, Evaluating Scour at Bridges, NH1-01-001. 4th Edition, Federal Highway Administration, 1988, Washington. DC.
[2] Laursen. E.M., Observations on the Nature of Scour, Proceedings of the Fifth Hydraulic Conference; Bulletin 34, University of Iowa, Iowa City, Iowa; June 9-11,1952, pp. 179-197.
[3] Meyer-Peter. E. and Muller. R., Formula for bed load transport, Proc. 2nd Meeting, Vol. 6, IAHR, Stockholm, 1948.
[4] Nielsen. P., Coastal bottom boundary layers and sediment transport, World Scientific, Singapore, 1992.
[5] Van Rijn. L. C., Sediment transport. Part II: suspended load transport, Journal of Hydraulic Engineering, 110-(11), 1984, pp. 1613–1641.
[6] Yang. S. Q., Formula for Sediment Transport in Rivers, Estuaries, and Coastal Waters, Journal of Hydraulic Engineering, 2005, pp. 968-978.
[7] Miller. W., Model for The Time Rate of Local Sediment Scour at A Cylindrical Structure, Dissertation, University of Florida, 2003, Florida.
[8] Natakusumah. D.K., Harlan. D., Herdiansyah. S.F., Local Scouring Around Pile and Curved Channel, International Journal of Geomate, Vol. 17, Issue 60, 2019, pp.1-8.
[9] Flow Science Team, Flow-3D User manual, Flow Science. Inc., 2008.
[10] Harlan. D., Natakusumah. D.K., Adityawan. M.B., Mahfudz. H., Adinata. F., 3D Numerical Modeling of Flow in Sedimentation Basin, MATEC Web of Conferences, 2018.
[11] Wei. G., Brethour. J., Grunzner. M., Burnham. J., The Sediment Scour Model in Flow-3D, Flow Science Report 03-14, 2014.
[12] Soulsby. R.L., Whitehouse. R.J.S.W., Threshold of Sediment Motion in Coastal Environments, Proceeding of Combined Australian Coastal Engineering and Port Conference, EA,1997, pp. 149-154.
[13] Breuser. H. N. C. and Raudviki. A.J., Scouring, IAHR Hydraulic Structure Design Manual, 1991, Rotterdam: AA Balkema.
[14] Chow. V.T., Open-Channel Hydraulics, McGraw-Hill, 1959, New York
[15] Soulsby. R., Dynamics of Marine Sands, Thomas Telford Publications, 1997, London.

[16] Winterwerp. J.C., Bakker. W.T., Mastbergen. D.R., Van Rossum. H., Hyperconcentrated sand-water mixture flows over erodible bed, Journal Hydraulics Engineering, Vol. 118, 1992, pp. 1508-1525.

[17] Richardson. E.V., Simons. D.B., and Julien. P.Y., Highway in the River Environment, Federal Highway Administration Publication FHWA – HI 90 – 106,1990, 719p.

[18] Laursen. E. M. and Toch, Scour Around Bridge Piers and Abutments, Iowa Highway, Res Board, Bulletin No.4, 1956, pp.60

[19] Melville. B.W. and Sutherland. A.J., Design Method for Local Scour at Bridge Piers. Journal of Hydraulic Engineering, Vol. 114, 1988, pp.1210-1226.

[20] Melville. B. W. and Raudkivi. A., Flow characteristics in local scour at bridge piers, J. Hydraul. Res., 15(4), 1977, pp. 373–380.